ELSEVIER

Journal of Archaeological Science 35 (2008) 302–309

Journal of Archaeological SCIENCE

http://www.elsevier.com/locate/jas

Roman blue-green bottle glass: chemical–optical analysis and high temperature viscosity modelling

P.A. Bingham [a,*], C.M. Jackson [b]

[a] *Department of Engineering Materials, University of Sheffield, Sir Robert Hadfield Building, Mappin Street, Sheffield, South Yorkshire S1 3JD, UK*

[b] *Department of Archaeology and Prehistory, University of Sheffield, Northgate House, West Street, Sheffield S1 4ET, UK*

Received 24 November 2006; received in revised form 9 February 2007; accepted 27 March 2007

Abstract

Chemical analysis, optical absorption spectroscopy and mathematical modelling of high temperature viscosity have been carried out on five 1st–2nd century AD Roman blue-green bottle glass fragments from Coppergate, York. Modelled viscosities indicate remarkable consistency within the sample set studied and support the suggestion that temperatures of ~1000–1150 °C were required to remelt these glasses and to provide suitable viscosities for forming articles. Iron redox ratios ($Fe^{2+}/\Sigma Fe$), analysed SO_3 contents and the absence of characteristic Fe^{3+}–S^{2-} amber absorption bands suggest that melting conditions for all studied glasses were mildly, rather than strongly, reducing (estimated $pO_2 \approx 10^{-1}$–10^{-6} bar). These furnace conditions are consistent with the effects of combustion gases and carbonaceous matter contained in the raw materials.

Keywords: Glass; Roman; Bottle; Viscosity; Modelling; Colour; Optical

1. Introduction

The discovery and spread of the technique of glass blowing throughout the Roman Empire enabled glass vessels to be produced cheaply and rapidly for the first time (Grose, 1989). Compared to the traditional methods of core forming and casting, free blowing and mould blowing were more efficient and hence more economical techniques. This contributed to the widespread manufacture of glass vessels from the middle of the 1st century AD (Foy and Sennequier, 1989). It is believed that glass vessels ceased to be purely luxury items and rapidly became more everyday in their use, for example as containers and tableware (Price, 1976; Grose, 1989). One of the newly-introduced vessel types was the blue-green square bottle, which is one of the most commonly encountered vessels of the 1st and 2nd Centuries AD, and which is thought to have been used for the storage and transportation of liquids (Charlesworth, 1966).

The composition of Roman glass is relatively stable and constant through time. This has led to the formation of two models for glass production during this period: (i) centralised production with local secondary working centres (e.g. Foy et al., 2000; Freestone et al., 2002) and (ii) dispersed production through local glass making and working centres (e.g. Wedepohl et al., 2003). In model (i), manufacture of glass from raw materials is considered to have taken place at large, centralised glassmaking facilities, mainly in the south-eastern Mediterranean, from whence the glass was transported to the provinces. Model (ii) suggests a large number of regional or local glassmakers, and compositional homogeneity arose through similar recipes or the trade in broken glass or cullet. The focus of the research which has given rise to these theories relates to discovering the provenance of Roman glass; glass technology has only been dealt within broad terms.

* Corresponding author. Tel.: +44 114 2225473; fax: +44 114 2225943.
E-mail address: p.a.bingham@sheffield.ac.uk (P.A. Bingham).

0305-4403/$ - see front matter © 2007 Elsevier Ltd. All rights reserved.
doi:10.1016/j.jas.2007.03.011

This paper seeks to explore aspects of the technology of Roman glass production relating to the melting characteristics of the glass and the extent to which the colour and working properties were controlled and influenced by Roman glass-makers. Roman blue-green bottles have been chosen because they form such a significant proportion of early assemblages, are relatively long-lived and represent glass which is unlikely to have been deliberately coloured. The glass is studied using modern spectroscopic and modelling techniques to gather information on raw materials and furnace conditions. Five glass samples originating from Roman blue-green square bottles found at Coppergate, York, have been examined in detail in this study. The glasses exhibit a range of colours from blue to green.

2. Experimental procedures

Five samples of blue-green bottle and mould-blown prismatic bottles from Coppergate, York were obtained for analysis. Sample designations are given as G+ small finds number, and variations in colour, assessed visually, are given in parentheses, G6106 (green), G13125 (blue), G3622 (blue-green), G14114 (blue) and G14131 (green).

Samples have been prepared for optical spectroscopy by grinding and polishing with successive SiC paper grades, followed by mechano-chemical polishing using aqueous CeO_2 suspension. Due to the origin of each sample and the requirement for their preservation, optical sample thicknesses vary from 2 mm to 4 mm. UV–Vis–IR spectra have been recorded in transmission mode from 295 nm to 3300 nm using a Perkin Elmer Lambda 2000 spectrometer. A monochromator change at 860 nm is responsible for slight inaccuracies at that wavelength, however, the effect is negligible in the context of this study. Measured transmission spectra have been corrected for reflection losses and converted to absorption using Eq. (1).

$$A = -\log \frac{I}{I_0(1-R)^2} \tag{1}$$

where A = absorption in cm^{-1}, I = transmitted intensity, I_0 = incident intensity, and R = reflection losses. Calculation of R has been made using Eq. (2), and by inputting published refractive indices (N) for glasses with compositions across the range studied here (Mazurin et al., 1987). This procedure indicates that a value of $R = 0.04$ is sufficiently accurate to be applied to all samples, since the small differences in R which do arise have a negligible effect upon corrected absorption spectra.

$$R = \left(\frac{N-1}{N+1}\right)^2 \tag{2}$$

Chemical analyses have been carried out on each sample using both inductively-coupled plasma-atomic emission spectroscopy (ICP-AES) and energy dispersive x-ray analysis (EDS) with a scanning electron microscope (SEM). ICP-AES analyses have been undertaken at the NERC ICP facility, Royal Holloway, University of London on a Perkin Elmer Optima 3300RL. Samples were digested in a hydrofluoric/perchloric acid mixture and reconstituted in 10% nitric acid solution, following the procedure for silicate rock dissolution given in Thompson and Walsh (1983). Silica is lost as silicon tetrafluoride during digestion and so is absent from the results: silica content has been assumed by difference and verified by EDS analysis. Al_2O_3, Fe_2O_3, MgO, CaO, Na_2O, K2O, TiO_2, P_2O_5, Sb_2O_3 and MnO have been measured and are given as oxides; Pb and other trace elements (the latter were not included in subsequent calculations) are presented in ppm. All elements have been corrected for drift using an in-house silicate rock standard. Accuracy associated with these measurements is estimated using a Corning B standard and is found to be, in absolute terms, ±5% for major elements and ±15% for the minor elements (measured below 1 wt%). Contents of Cl and S (expressed as SO_3) cannot be measured by ICP-AES, so SEM-EDS analysis has been utilised to detect these components. SEM samples are prepared by setting in resin, then using the same grinding/polishing regime as for optical spectroscopy sample preparation. Material bulk compositions have been analysed using a Link EDS unit fitted to a Philips 500 SEM. Three measurements are made at separate points on each sample, which are then averaged. Errors associated with EDS measurements of SO_3 and Cl are estimated to be ±0.1 wt% and ±0.2 wt%, respectively.

The iron redox ratio $Fe^{2+}/\Sigma Fe$ has been estimated using an established optical method (Adès et al., 1990; Schreurs and Brill, 1984). The maximum spectral absorbance of the peak centred at ~1075 nm, which has been widely attributed to Fe^{2+} cations occupying a range of distorted octahedral sites (Adès et al., 1990; Edwards et al., 1972; Bates, 1962), has been obtained for each sample by optical absorption spectroscopy. Calibration is provided using measured peak absorbances for two samples similar in composition to those studied here (nominal wt% 69.94 SiO_2, 15.50 Na_2O, 14.03 CaO, 0.53 Fe_2O_3), and for which the iron redox ratio has been measured. These two glasses were melted in gas-fired and electric furnaces that provided substantially different oxygen partial pressures (pO_2). The iron redox ratio was then measured for each sample using a wet chemical technique (Jones et al., 1981), producing values of $Fe^{2+}/\Sigma Fe = 0.16$ and 0.40. Using the measured absorbance at peak maximum (~1075 nm) for both samples, a calibration graph has been obtained which allows quantification of the optically-detected $Fe^{2+}/\Sigma Fe$ ratio. This method makes the following assumptions: (i) all Fe contents fall within the limits of applicability of Beer's Law; (ii) the only contribution to the peak at ~1075 nm arises from Fe^{2+}; (iii) Fe^{2+} extinction coefficients remain unchanged; and (iv) the fraction of Fe^{2+} cations that are octahedrally coordinated remains constant for all samples and calibration glasses. Taking into account these assumptions, estimated errors for optically-detected $Fe^{2+}/\Sigma Fe$ are ±0.05 (i.e. ±5% error in $Fe^{2+}/\Sigma Fe$ ratio).

High temperature viscosity has been estimated for the glass samples shown in Table 1 using the Vogel-Fulcher-Tammann (VFT) Eq. (3), which relates glass viscosity to temperature for a Newtonian fluid.

Table 1
Sample analyses, estimated redox ratios and predicted viscosities

	G6106	G13125	G3622	G14114	G14131
SiO_2/wt%	69.0	69.0	69.4	69.4	67.1
Al_2O_3/wt%	2.3	2.6	2.3	2.1	2.6
Fe_2O_3/wt%	0.49	0.64	0.80	0.74	0.33
MgO/wt%	0.49	0.59	0.48	0.47	0.55
CaO/wt%	6.2	6.7	6.3	6.0	9.3
Na_2O/wt%	18.2	17.3	17.4	18.2	16.6
K_2O/wt%	0.52	0.74	0.54	0.50	0.52
TiO_2/wt%	0.08	0.10	0.08	0.08	0.05
P_2O_5/wt%	0.09	0.12	0.10	0.09	0.08
MnO/wt%	0.35	0.51	0.46	0.37	0.92
SO_3/wt%	0.37	0.22	0.36	0.30	0.23
Cl/wt%	1.4	1.1	1.2	1.2	1.6
Sb_2O_3/wt%	0.37	0.28	0.35	0.43	0.00
Co/ppm	3	4	6	4	8
Cr/ppm	16	17	16	16	12
Cu/ppm	39	109	64	48	21
Li/ppm	4	13	6	4	1
Ni/ppm	9	11	11	10	19
Sc/ppm	1	1	1	1	1
V/ppm	10	15	15	10	14
Y/ppm	8	9	8	8	10
Zn/ppm	23	30	31	29	25
Sr/ppm	428	474	411	388	725
Ba/ppm	210	263	223	207	275
Pb/ppm	227	231	272	206	6
$(Fe^{2+}/\Sigma Fe) \pm 0.05$	0.25	0.35	0.37	0.34	0.33
$T\log(\eta/\text{dPa s}) = 2/°C$	1394	1409	1407	1399	1363
$T\log(\eta/\text{dPa s}) = 3/°C$	1113	1127	1125	1116	1103
$T\log(\eta/\text{dPa s}) = 4/°C$	956	970	966	958	954
$T\log(\eta/\text{dPa s}) = 5/°C$	837	850	848	839	835
$T\log(\eta/\text{dPa s}) = 6/°C$	753	764	764	754	767
$T\log(\eta/\text{dPa s}) = 7.6/°C$	663	673	672	664	679
Working range/°C	293	297	294	294	275

$$\log \eta = A + \frac{B}{T - T_0} \tag{3}$$

where η = viscosity, A and B and T_0 are constants and T = temperature. The constants A, B and T_0, which are calculated using contributions from each component oxide, have been evaluated and validated using measured viscosities for silicate glasses similar in composition to those studied here (Lakatos et al., 1972, 1975; Lakatos, 1976; Lakatos and Johansson, 1977; Bingham and Marshall, 2005). We have further validated the applicability of Lakatos' method to Roman blue-green glass by modelling the viscosities of 12 glasses with compositions falling across the same range as the Roman glasses (wt%: SiO_2, 65–73; Na_2O, 13–21; CaO, 5–10; MgO, 0–3; K_2O, 0–2; Al_2O_3, 0–3) and for which viscosities have been measured (Mazurin et al., 1987). Modelled temperatures corresponding to viscosities throughout the range $\log(\eta/\text{dPa s}) = 2$–6 are within 15 °C of measured values in 11 out of 12 cases. Moreover, it is noted that the majority of viscosity measurements have been made using rotating viscometers. Even state-of-the-art viscosity measurement techniques carry errors of 3–4 °C at elevated temperatures (Bose et al., 2001). The errors associated with older measurements may well be larger. As a result of our validation investigations we have therefore concluded that high temperature viscosities of our Roman blue-green glass compositions can be modelled with sufficient confidence in their accuracy by using Lakatos' values of A, B and T_0. Furthermore, this methodology may be more widely applicable to ancient glasses. It has been necessary to make certain simplifications owing to the absence of mathematical factors for some of the more minor components. Where possible, calculations have been made using components producing closely similar viscosity behaviour. The contents of Cl, Sb_2O_5, MnO, Fe_2O_3, SO_3, TiO_2 and trace elements have been omitted, and for the purposes of modelling, *pro rata* multiplication of the composition to total 100% has been made. This has been taken into account when estimating errors, which are as follows: ±20 °C at $\log(\eta/\text{dPa s}) = 2$, decreasing linearly with increasing $\log \eta$, to reach a value of ±15 °C at $\log(\eta/\text{dPa s}) = 7.6$.

3. Results and discussion

3.1. Composition and modelled high temperature viscosity

The chemical analysis results shown in Table 1 demonstrate that the Coppergate glass compositions studied here are low magnesia glasses, typical of Roman blue-green square bottles in terms of their major constituent (SiO_2, Na_2O, CaO) and MgO, K_2O, Al_2O_3, Fe_2O_3 and P_2O_5 contents. These glasses occur in a tightly-controlled compositional region, also typical of many ancient and historic glasses. Modelling of high temperature viscosity of historic glasses has received little interest (Fischer and McCray, 1999); however, it can provide insight into furnace temperatures and working properties without the requirement for direct measurement of the glasses or facsimiles thereof. The working range, or the range of temperatures within which the glass is sufficiently fluid to be worked or formed into shapes, occurs for SiO_2–Na_2O–CaO glasses between the working point, $\log(\eta/\text{dPa s}) = 4$, and the softening point, $\log(\eta/\text{dPa s}) = 7.6$. At lower viscosities the glass is too fluid to hold a shape, and near to and below the softening point the glass no longer flows sufficiently and cannot be worked. Modelled high temperature viscosities for the samples studied here are listed in Table 1 and illustrated in Fig. 1. The five blue-green glasses from Coppergate exhibit similar working points ($\log(\eta/\text{dPa s}) = 4$ varies by only 16 °C). Silica contents remain within tightly-controlled limits (~69–71 wt%), and ($Na_2O + CaO$) content is 24.0–25.8 wt%. Since Na_2O and CaO have broadly similar (but not identical) effects on high temperature viscosity, this has a smoothing effect such that high temperature viscosities remain closely similar and the glasses display a remarkable consistency in their working range (the temperature difference between $\log(\eta/\text{dPa s}) = 4$ and $\log(\eta/\text{dPa s}) = 7.6$). Sample G14131 is slightly "shorter" than the other four glasses owing to its higher CaO content, yet even this sample exhibits a working range only ~20 °C smaller than the other samples.

Earlier predictions of melting temperatures of Roman glasses give a range of temperatures from 1000 °C to 1200 °C

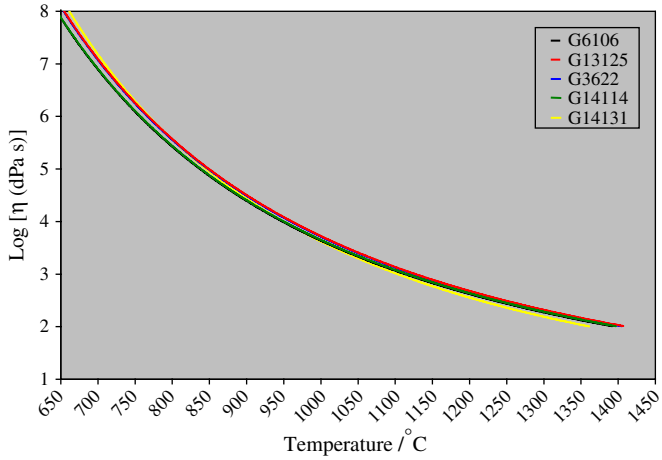

Fig. 1. Modelled high temperature viscosity profiles.

for either glass production or for remelting glass. Following the discovery of potential glass making at Coppergate, York, temperature estimates based upon the temperature ranges of quartz transformation states in glassy waste, together with the vitrification structures observed in the glass melting pots, indicated that temperatures of 1200 °C were reached (Jackson et al., 2003). Brill (1963) suggested that a workable "Roman-type" soda-lime-silica batch-free glass could be produced at temperatures in excess of 1100 °C. Brill (1988) also concluded on the basis of measured glass viscosities that glass originating from Jalame in Palestine, and which is broadly similar in composition to Roman blue-green glass, had to achieve 1000–1100 °C in order to be worked. It has been demonstrated experimentally that Egyptian-style glass furnaces, dating to the second millennium BC, could attain temperatures in excess of 1150 °C (Jackson et al., 1998), so there is no reason to suggest that Roman furnaces were any less technologically sophisticated. The viscosity of a glass does not directly indicate the temperatures required for melting from batch, given that the initial chemical reactions, homogenisation and refining may require higher temperatures and/or longer melting times to achieve a batch-free, refined glass (Preston and Turner, 1940). However, viscosity does indicate the temperatures that are necessary to remelt from raw glass or cullet and subsequently to work the glass. Our modelled viscosities indicate working ranges of ~660–970 °C. Assuming that glasses were remelted from fully formed glass (raw glass or cullet) rather from primary raw materials, modelled viscosities support the suggestion that these glasses could be melted, homogenized and refined at temperatures of ~1000–1150 °C, given sufficient time-at-temperature. Furnace temperatures below 1000 °C would have made it more difficult to melt these glasses, to remove bubbles from the melts, and to subsequently gather the molten glass prior to hot working.

3.2. Melting, homogenization and refining

Temperatures of ~1000–1150 °C correspond to melt viscosities in the region of $\log(\eta/\mathrm{dPa\ s}) = 2.8–3.4$ for Roman blue-green glass, indicating that a period of many hours could have been required to homogenise and refine the glass to achieve the quality that has been observed. Homogenisation and refining may have been aided by a number of the glass constituents. The use of compounds of Sb, Mn, S and Cl can be expected to have provided some degree of refining and homogenization during melting. This would have enhanced glass quality and bubble removal and potentially decreased furnace residence times.

Refining is the removal of bubbles, a process involving mass transfer, bubble growth and rise to the surface or dissolution in the melt. Bubble rise can be described by buoyancy effects and therefore by Stokes' law, which can be rearranged to give Eq. (4).

$$V_b = \frac{g\Delta\rho r^2}{3\eta} \tag{4}$$

where V_b = rate of rise of the bubble, g = gravitational acceleration, $\Delta\rho$ = difference in density between sphere and liquid, r = radius of sphere and η = viscosity of liquid. Bubble removal is facilitated by a low melt viscosity and a large bubble diameter. Bubbles arise from gases (primarily CO_2) trapped during the early stages of melting, but also from gases released during melting which are caused by chemical interactions and redox effects.

Antimony provides a useful combination of high temperature oxidising (Weyl, 1951; Schreiber et al., 1990) and refining (Volf, 1984; Shelby, 1997) actions due to low temperature batch reactions occurring early in melting Eq. (5), followed by the release of O_2 at high melting temperatures due to thermal decomposition Eq. (6).

$$O_2\ (\text{batch}) + Sb_2O_3 \rightarrow Sb_2O_5 \tag{5}$$

$$Sb_2O_5 \rightarrow Sb_2O_3 + O_2\uparrow \tag{6}$$

Roman glassmakers derived Sb from minerals, with stibnite (Sb_2S_3) one possible source (Jackson, 2005). In addition to the refining action of antimony (once converted during melting from antimony sulphide to antimony oxide) the presence of sulphide may also have provided beneficial refining effects. The use of stibnite as the source of Sb, which may be suggested by trace element analysis, could have provided further advantages in terms of refining over the use of an oxide-based Sb raw material. However, the use of a sulphide raw material could have resulted in more reducing conditions (DiBello, 1989). The presence of Sb in the bottle glasses analysed here probably derives from glass recycling.

The addition of MnO_2 as an oxidising agent for the production of ancient glasses has been suggested (Volf, 1984; Schreurs and Brill, 1984; Green and Hart, 1987). However, as summarised by Jackson (2005), it has also been suggested that Mn may have originated from the sands used at the time; from recycling; or from the use of glassmaker's soap. The deliberate addition of MnO_2 would not only decolourise the glass by mutual redox interactions with Fe (discussed in Section 3.3), but also produce refining due to the liberation

of oxygen at elevated temperatures. As little as 0.5% MnO_2 can be an effective refining agent (Volf, 1984). Given the Mn content of our Sb-free glass G14131, this glass probably contained deliberate additions of Mn.

Sulphates and chlorides provide low temperature liquid phases that act as melt accelerants by dissolving sand grains early in the melting process (Shelby, 1997). As the SiO_2 content of these phases increases their SO_3 solubility decreases, releasing SO_3 into the melt, which decomposes to form O_2 and SO_2 as in Eq. (7).

$$2SO_3\,(\text{melt}) \rightarrow 2SO_2 + O_2\uparrow \qquad (7)$$

In turn the SO_2 and O_2 dissolve in the melt or rise to the surface, aiding refining as described in Eq. (4). Sulphur solubility in a silicate melt is dictated by glass composition, melting temperature and the oxygen partial pressure, pO_2, in the furnace. Given that the compositions of the Coppergate glasses are closely similar, compositional effects on residual S content are small. Temperature (Nagashima and Katsura, 1973; Schreiber et al., 1990) and pO_2 (Beerkens and Kahl, 2002; DiBello, 1989; Nagashima and Katsura, 1973; Schreiber et al., 1990) have stronger effects on S content, with pO_2 dominant within the range of temperatures considered here. Typical upper limits in the Cl content of technological (Bateson and Turner, 1939) and archaeological (Gerth et al., 1998) SiO_2-Na_2O-CaO glasses are 1–1.5 wt%. Unlike F, which substitutes in the network in significant quantities for O, Cl does so only at low levels. This difference in behaviour can be attributed to the similarity in ionic radii between F^- and O^{2-} which does not exist between Cl^- and O^{2-} (Volf, 1984). Sodium chloride (<2 wt%) has been used as a refining agent in modern SiO_2–Na_2O–CaO glass manufacture (Volf, 1984), in which it decreases melt surface energies and promotes melting by increasing wetting of batch particles. The combination of NaCl with Na_2CO_3 provides a eutectic mixture whose melting point is 838 °C; 213 °C below the melting point of Na_2CO_3. This eutectic mixture therefore reacts more rapidly with sand grains, effectively increasing melting rates. Of particular relevance to ancient glass making, it has been noted that the chloride refining effect occurs intensely in the temperature range 1100–1200 °C (Volf, 1984), which is consistent with the range of temperatures that we suggest were required to re-melt the Coppergate blue-green bottle glass samples.

3.3. Optical properties and redox conditions

Iron, the chief colourant in Roman blue-green glass, was probably not an intentional batch addition but was a natural component of the sands used at the time (Turner, 1956; Brill, 1988; Silvestri et al., 2006). To manufacture colourless or decolourised glass, the glassmaker had to add decolourising agents, specifically Mn and/or Sb (Sayre, 1963). Iron occurs in most silicate glasses simultaneously in two oxidation states: Fe^{2+} and Fe^{3+}. The ratio $Fe^{2+}/\Sigma Fe$ is crucial in determining the colour: a reduced glass with a higher $Fe^{2+}/\Sigma Fe$ exhibits a strong blue colour, but if $Fe^{2+}/\Sigma Fe$ is low, this produces a weaker yellow-green colour. Low $Fe^{2+}/\Sigma Fe$ is therefore favourable if one is seeking to minimise the colour of iron-containing glasses. Two Fe^{2+} absorption bands are expected, corresponding to $^5T_2(D) \rightarrow {}^5E(D)$ and $^5E(D) \rightarrow {}^5T_2(D)$ transitions for octahedrally and tetrahedrally-coordinated Fe^{2+}, respectively (Bates, 1962; Adès et al., 1990; Edwards et al., 1972). These bands occur in silicate glasses at ~1075 nm (octahedral, with a broad tail that continues into the red-visible portion of the spectrum and hence the blue colour of Fe^{2+} in glass), and at ~2000 nm (tetrahedral). The Fe^{3+} and Mn^{2+} ions both have the same $3d^5$ electronic configuration, for which all d–d transitions are forbidden, decreasing their intensity considerably. The $3d^5$ configuration produces a complex range of weak, narrow absorption bands in the same narrow range of 330–625 nm (Bates, 1962; Hannoyer et al., 1992; Nelson and White, 1980). Bands have been observed at 380 nm, 415 nm, 435 nm, 445 nm and 490 nm due to Fe^{3+} and at 352 nm and 422 nm due to Mn^{2+}. Absorption bands characteristic of Fe^{2+}, Fe^{3+} and Mn^{2+} are evident in all spectra shown in Figs. 2 and 3. Absorption due to Mn^{3+}, which has the $3d^4$ electronic configuration, produces a purple colouration in glass. This is due to broad absorption centred at ~500 nm, and has been observed in some archaeological glasses (Sanderson and Hutchings, 1987). It is attributable to the spin-allowed $^5E(D) \rightarrow {}^5T_2(D)$ transition for octahedrally coordinated Mn^{3+} (Nelson and White, 1980). Any Mn^{3+} that may be present in our sample glasses occurs at low concentrations, as evidenced by the weakness of absorption at ~500 nm. Small absorption bands highlighted in Fig. 3 and occurring at ~535 nm and ~590 nm cannot be unambiguously attributed given the available information. However, it is possible that small concentrations of Mn^{3+}, Cr^{3+}, Co^{2+} and/or Ni^{2+} could contribute to absorption at these wavelengths (Bates, 1962). Whilst Cr^{3+}, Ni^{2+} and Co^{2+} are only present at ppm levels (3–19 ppm), Ni^{2+} and Co^{2+} in particular produce intense absorption bands (Bates, 1962).

Mutual redox interactions can occur between multivalent elements in silicate melts (Schreiber, 1987). Stoichiometric reactions may take place between elements whose reduction

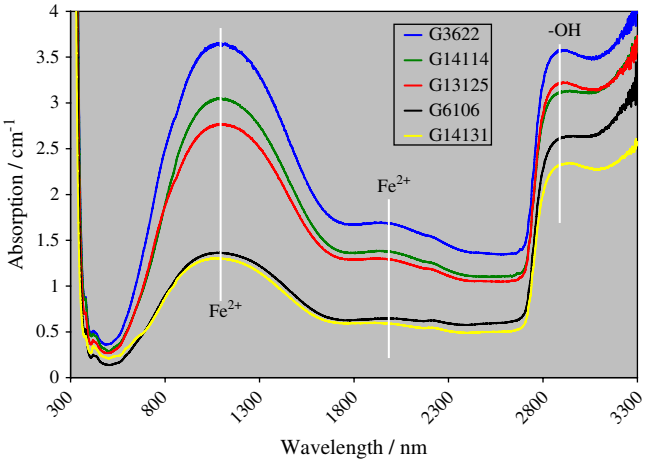

Fig. 2. Reflection-corrected, normalised optical absorption spectra.

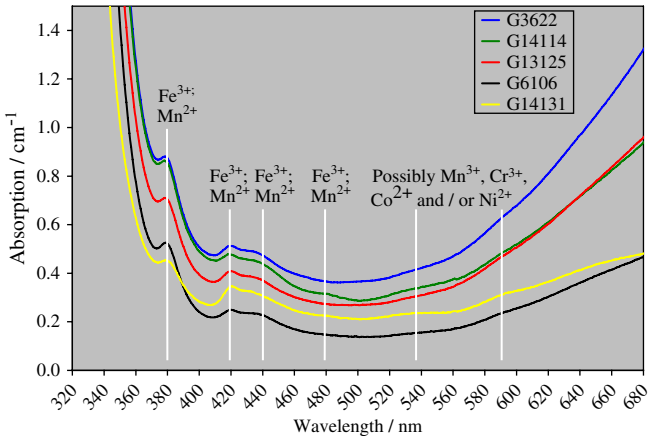

Fig. 3. Reflection-corrected, normalised visible wavelength optical absorption spectra.

potentials are sufficiently different; however, partial or no reaction may occur between elements with more similar reduction potentials. For example, the Fe^{3+}/Fe^{2+} and Mn^{3+}/Mn^{2+} reference reduction potentials in sodium silicate glass at 1085 °C are 0.7 and −2.1, respectively. The difference between potentials is large $[0.7-(-2.1)]=2.8$, so iron and manganese, if no other multivalent species are present, should normally undergo stoichiometric or nearly stoichiometric redox interactions which cause the reaction described in Eq. (8) to proceed to the right (Schreiber, 1987).

$$Fe^{2+}+Mn^{3+}\leftrightarrow Fe^{3+}+Mn^{2+} \quad (8)$$

This has the effect of causing the $Fe^{2+}/\Sigma Fe$ ratio to approach 0 and the $Mn^{2+}/\Sigma Mn$ ratio to approach 1, simultaneously increasing the proportions of the weakly-colouring $3d^5$ ions present in the glass. However, in the Roman glasses under consideration, a number of factors combine to prevent this reaction from proceeding to completion. At least one of two other multivalent elements, S and Sb, are present at concentrations of the same order as Fe and Mn, and must therefore be taken into consideration, in addition to the effects of temperature and oxygen partial pressure (pO_2) during melting, and redox equilibrium having not been attained. The reference reduction potential of Sb^{3+}/Sb^{5+} is −0.9, which is intermediate between those of Mn^{2+}/Mn^{3+} and Fe^{2+}/Fe^{3+}. On this basis alone one might suspect Sb to be less effective than Mn at oxidising Fe. However, since the oxidation/reduction of Sb^{3+}/Sb^{5+} is a two-electron process, it is more sensitive to changes in pO_2 (Schreiber, 1987). As a result, under mildly reducing pO_2 (see below), Sb can become as strongly reduced as Mn, and in doing so releases twice as many electrons in the process (Schreiber, 1987). This is consistent with previous works which indicate that Sb is a stronger or more important decolouriser than Mn (see, for example, Jackson, 2005; Weyl, 1951). Redox potential alone does not dictate the effectiveness of an oxidant: the form in which the oxidant is introduced to the melt, the furnace temperature, pO_2 and glass composition are also involved. Redox equilibrium does not occur in ancient glasses, and as a result the various mutual redox interactions which can take place are only partially complete. Redox potentials, therefore, have only been used in this study as guidelines rather than quantitative expressions to explain the redox behaviour.

The combined presence of Fe^{3+} and S^{2-}, which can occur in silicate melts prepared under strongly reducing conditions ($pO_2 < \sim 10^{-6}$ bar) (Beerkens and Kahl, 2002; DiBello, 1989) gives rise to an intense and characteristic "amber" colouration (Beerkens and Kahl, 2002; DiBello, 1989; Schreurs and Brill, 1984; Green and Hart, 1987; Douglas and Zaman, 1969). This amber colour is the result of increased UV absorption which shifts the UV edge to longer wavelengths, and to the development of a new absorption band centred at ~410 nm, which has been attributed to tetrahedrally-coordinated Fe^{3+} ions surrounded by three O^{2-} ions and one S^{2-} ion (Schreiber et al., 1990). The amber chromophore has been analysed in ancient glasses (Schreurs and Brill, 1984), in modern commercial glasses (Douglas and Zaman, 1969) and in glasses for nuclear waste immobilization (Schreiber et al., 1990). Analysis of our spectra and comparison with published amber glass spectra confirms the absence of the amber chromophore in the Coppergate glasses. It is therefore concluded that no detectable levels of S^{2-} are present in the five Coppergate glasses.

The coexistence of S^{6+} and S^{2-} species only occurs under highly reducing conditions ($pO_2 = 10^{-9}-10^{-11}$ bar in borosilicate glass at 1150 °C) (Schreiber et al., 1987, 1990). Therefore redox interactions are not expected to involve S when $pO_2 > \sim 10^{-6}$ bar. Given that sulphur remains in the S^{6+} state under all but the most strongly reducing conditions, and given that the logarithm of its solubility is proportional to pO_2 (Nagashima and Katsura, 1973; Schreiber et al., 1990), the sulphur content of glass can be used as an approximate guide to pO_2 in the furnace in which it was melted. The measured SO_3 contents of the five Coppergate glasses (~0.2–0.4 wt% SO_3), combined with our estimation of their melting temperatures (~1000–1150 °C) correspond with pO_2 in the range $\sim 10^{-1}-10^{-6}$ bar, based on data for sodium silicate (Nagashima and Katsura, 1973) and borosilicate (Schreiber et al., 1987) glasses, and upon measured iron redox ratios (Schreiber, 1987). It therefore also follows that furnace pO_2 during initial melting from batch must have been greater than $\sim 10^{-6}$ bar, because at pO_2 values below $\sim 10^{-6}$ bar the residual SO_3 content would approach its minimum (<0.1 wt%) (Beerkens and Kahl, 2002; Schreiber et al., 1987).

For sample G14131, which contains no Sb_2O_3 and an excess of Mn relative to Fe, decolourisation should be adequately described by Eq. (8) proceeding fully to the right. However, the measured $Fe^{2+}/\Sigma Fe$ ratio of 0.33 demonstrates that Eq. (8) did not proceed to completion, underlining the complexity of melting conditions and indicating the presence of reducing conditions. Given the difficulty in extracting useful information from the two-component redox system of sample G14131 (Fe + Mn), it is clearly not feasible to do so for the three-component systems (Fe + Mn + Sb), other than in general terms. It is noted that Mn + Sb occurs in molar excess to Fe for all five samples. However, as with sample G14131,

less than full oxidation of Fe occurred. Brill (1988) noted similar difficulties in separating the effects of furnace atmosphere and batch ingredients on redox of ancient glasses. The Coppergate samples are more strongly oxidised ($Fe^{2+}/\Sigma Fe = 0.25$–0.37) than blue-green glass obtained from a 4th century AD glass factory at Jalame ($Fe^{2+}/\Sigma Fe = 0.64$) (Schreurs and Brill, 1984; Brill, 1988). However, the Coppergate glasses contain an excess of oxidising agents such that $(Mn + Sb) > Fe$, whereas the Jalame glass does not $(Mn + Sb) \ll Fe$. Assuming that the Coppergate and Jalame samples did not experience a grossly dissimilar furnace temperature or pO_2, the measured differences in redox are consistent with the higher $(Mn + Sb)$ contents of the Coppergate glasses.

4. Conclusions

Analysis of five 1st–2nd century AD Roman blue-green bottle fragments from Coppergate, York has indicated close compositional grouping resulting in repeatable high temperature working properties. For the first time, our combined approach has allowed estimation of furnace pO_2 for Roman blue-green glasses. High temperature viscosities for these and for other blue-green glasses have been modelled using established techniques. Results support previous suggestions that furnace temperatures of 1000–1150 °C were used to remelt Roman blue-green glass. Optical analysis demonstrates moderate (25–37%) values of the iron redox ratio, $Fe^{2+}/\Sigma Fe$. Given the presence of a molar excess of $(Mn + Sb)$ to Fe in all cases, the measured levels of Fe^{2+} in combination with SO_3 contents and the absence of the Fe^{3+}–S^{2-} amber chromophore, support the suggestion that mildly reducing ($pO_2 \sim 10^{-1}$ to 10^{-6} bar) melting conditions occurred. These conditions would act in opposition to the oxidative decolourisation of Fe by $(Mn + Sb)$. These findings have implications for archaeological studies relating to Roman glass technology, and especially for our understanding of the conditions required for reworking raw glass or glass recycling.

Acknowledgements

The authors would like to acknowledge with thanks the efforts of Mihalis Catapotis, who laid the foundations upon which the work presented here has been built (glass project for the M.Sc Archaeomaterials, University of Sheffield). Thanks also are given to York Archaeological Trust for donating the bottle glass.

References

Adès, C., Toganidis, T., Traverse, J.P., 1990. High temperature optical spectra of soda-lime-silica glasses and modelization in view of energetic applications. J. Non-Cryst. Solids 125, 272–279.

Bates, T., 1962. Ligand field theory and absorption spectra of transition metal ions in glass. In: Mackenzie, J.D. (Ed.), Modern Aspects of the Vitreous State, vol. 2. Butterworths, London.

Bateson, H.M., Turner, W.E.S., 1939. A note on the solubility of sodium chloride in a soda-lime-silica glass. J. Soc. Glass Technol. 23, 265T–267T.

Beerkens, R.G.C., Kahl, K., 2002. Sulfur chemistry in soda lime silica glass melts. Phys. Chem. Glasses. 43, 189–198.

Bingham, P.A., Marshall, M., 2005. Reformulation of container glasses for environmental benefit through lower melting temperatures. Glass Technol. 46, 11–19.

Bose, N., Klingenberg, G., Meerlender, G., 2001. Viscosity measurements of glass melts – certification of reference material. Glass Sci. Technol. Glastech. Ber. 74, 115–126.

Brill, R.H., 1963. Ancient glass. Sci. Am. 209, 120–132.

Brill, R.H., 1988. Scientific investigations of the Jalame glass and related finds. In: Weinberg, G.D. (Ed.), Excavations at Jalame, Site of a Glass Factory in Late Roman Palestine. Univ. Missouri Press, Columbia, USA.

Charlesworth, D., 1966. Roman square bottles. J. Glass Stud. 8, 26–40.

DiBello, P.M., 1989. Controlling the oxidation state of a glass as a means of optimising sulphate usage in melting and refining. Glass Technol. 30, 160–165.

Douglas, R.W., Zaman, M.S., 1969. The chromophore in iron–sulphur amber glass. Phys. Chem. Glasses. 10, 125–132.

Edwards, R.J., Paul, A., Douglas, R.W., 1972. Spectroscopy and oxidation–reduction of iron in $MO.P_2O_5$ glasses. Phys. Chem. Glasses 13, 137–143.

Fischer, A., McCray, W.P., 1999. Glass production activities as practised at Sepphoris, Israel (37 BC–AD 1516). J. Archaeol. Sci. 26, 893–905.

Foy, D., Sennequier, G., 1989. Ateliers du verriers de l'antiquité à la period préindustrielle. In: Actes du 4e Rencontres d'Association Française pour de l'Archéologie du Verre. Rouen, 1991, pp.13–30 and 35–69.

Foy, D., Vichy, M., Picon, M., 2000. Lingots de verre en Méditerranée occidentale (IIIe siècle av. J.-C. - VIIe siècle ap. J.-C.). In: Annales du 14e Congrès de l'Association Internationale pour l'Histoire du Verre, Venezia-Milano 1998. AIHV, Lochem, pp. 51–57.

Freestone, I.C., Ponting, M., Hughes, M.J., 2002. The origins of Byzantine glass from Maroni Petrera, Cyprus. Archaeometry 44, 257–272.

Gerth, K., Wedepohl, K.H., Heide, K., 1998. Experimental melts to explore the technique of Medieval woodash glass production and the chlorine content of Medieval glass types. Chemie der Erde 58, 219–232.

Green, L.R., Hart, F.A., 1987. Colour and chemical composition in ancient glass: an examination of some Roman and Wealden glass by means of ultraviolet-visible-infrared spectrometry and electron microprobe analysis. J. Archaeol. Sci. 14, 271–282.

Grose, D.F., 1989. Early Ancient Glass. Core-Formed, Rod-Formed, and Cast Vessels and Objects from the Late Bronze Age to the Early Roman Empire, 1600 B.C. to A.D. 50. Hudson Hills Press, New York.

Hannoyer, B., Lenglet, M., Dürr, J., Cortes, R., 1992. Spectroscopic evidence of octahedral iron (III) in soda-lime-silicate glasses. J. Non-Cryst. Solids 151, 209–216.

Jackson, C.M., 2005. Making colourless glass in the Roman period. Archaeometry 47, 763–780.

Jackson, C.M., Nicholson, P.T., Gneisinger, W., 1998. Glassmaking at Tell el-Amarna: an integrated approach. J. Glass Stud. 40, 11–23.

Jackson, C.M., Wager, E.C.W., Joyner, L., Day, P.M., Booth, C.A., Kilikoglou, V., 2003. Roman Glass-making at Coppergate, York? Analytical evidence for the nature of production. Archaeometry 45, 445–466.

Jones, D.R., Jansheski, W.C., Goldman, D.S., 1981. Spectrophotometric determination of reduced and total iron in glass with 1,10 phenanthroline. Anal. Chem. 53, 923–924.

Lakatos, T., Johansson, L.-G., Simmingsköld, B., 1972. Viscosity temperature relations in the glass system SiO_2–Al_2O_3–Na_2O–K_2O–CaO–MgO in the composition range of glasses. Glass Technol. 13, 88–95.

Lakatos, T., Johansson, L.-G., Simmingsköld, B., 1975. Influence of Li_2O and B_2O_3 on the viscosity of soda-lime-silica glass. Glastek. Tidskr. 30, 7–8.

Lakatos, T., 1976. Viscosity–temperature relations in glasses composed of SiO_2–Al_2O_3–Na_2O–K_2O–Li_2O–CaO–MgO–BaO–ZnO–PbO–B_2O_3. Glastek.Tidskr. 31, 51–54.

Lakatos, T., Johansson, L.G., 1977. SiO_2–Al_2O_3–Na_2O–K_2O–CaO–MgO-systemets viskositet, likvidustemperatur och hydrolytiska resistens. Glastek. Tidskr. 32, 31–35.

Mazurin, O.V., Streltsina, M.V., Shvaiko-Shvaikovskaya, T.P., 1987. Handbook of Glass Data, Part C: Ternary Silicate Glasses. Elsevier, Oxford.

Nagashima, S., Katsura, T., 1973. The solubility of sulfur in Na_2O-SiO_2 melts under various oxygen partial pressures at 1100 °C, 1250 °C and 1300 °C. Bull. Chem. Soc. Jpn. 46, 3099–3103.

Nelson, C., White, W.B., 1980. Transition metal ions in silicate melts – I. Manganese in sodium silicate melts. Geochim. Cosmochim. Acta. 44, 887–893.

Preston, E., Turner, W.E.S., 1940. Fundamental studies of the glass melting process. The effect of particle size and temperature on the rate of glass formation of a pure soda-lime-silica glass. J. Soc. Glass Technol. 24, 124–138.

Price, J., 1976. Glass. In: Strong, D., Brown, D. (Eds.), Roman Crafts. Duckworth, London, pp. 110–125.

Sanderson, D.C.W., Hutchings, J.B., 1987. The origins and measurement of colour in archaeological glasses. Glass Technol. 28, 99–105.

Sayre, E.V., 1963. The intentional use of antimony and manganese in ancient glasses. In: Matson, F.R., Rindone, G. (Eds.), Advances in Glass Technology. Part 2. Plenum Press, New York, pp. 263–282 (see page 280 also Figs. 11, 12).

Schreiber, H.D., 1987. An electrochemical series of redox couples in silicate melts: a review and applications to geochemistry. J. Geophys. Res. 92, 9225–9232.

Schreiber, H.D., Kozak, S.J., Leonhard, P.G., McManus, K.K., 1987. Sulfur chemistry in a borosilicate melt. Part 1. Redox equilibria and solubility. Glastech. Ber. 60, 389–398.

Schreiber, H.D., Kozak, S.J., Schreiber, C.W., Wetmore, D.G., Riethmiller, M.W., 1990. Sulphur chemistry in a borosilicate melt. Part 3. Iron–sulphur interactions and the amber chromophore. Glastech. Ber. 63, 49–60.

Schreurs, J.W.H., Brill, R.H., 1984. Iron and sulphur related colours in ancient glass. Archaeometry 26, 199–209.

Shelby, J.E., 1997. Introduction to Glass Science and Technology. Royal Society of Chemistry, Cambridge, UK.

Silvestri, A., Molin, G., Salviulo, G., Schievenin, R., 2006. Sand for Roman glass production: an experimental and philological study on source of supply. Archaeometry 48, 415–432.

Thompson, M., Walsh, J.N., 1983. A Handbook of Inductively Coupled Plasma Spectrometry, first ed. Blackie & Son, Glasgow.

Turner, W.E.S., 1956. Studies in ancient glasses and glassmaking processes, Part V: raw materials and melting processes. J. Soc. Glass Technol. 40, 277T–300T.

Volf, M.B., 1984. Chemical Approach to Glass. Elsevier, Amsterdam, Netherlands.

Wedepohl, K.H., Gaitzsch, W., Follmann-Schultz, A.B., 2003. Glassmaking and glassworking in six Roman factories in the Hamback Forest, Germany. In: Annales du 15e Congrès del'Association Internationale pour l'Histoire du Verre, Corning, New York, 2001. AIHV, Nottingham, pp. 56–61.

Weyl, W.A., 1951. Coloured Glasses. Society of Glass Technology, Sheffield.